Proceedings of the
46th IEEE Conference on Decision and Control
New Orleans, LA, USA, Dec. 12-14, 2007

A Multi-Component Spatially-Distributed Model of Two-Phase Flow for Estimation and Control of Fuel Cell Water Dynamics

B.A. McCain and A.G. Stefanopoulou and I.V. Kolmanovsky

Abstract— **The critical task of controlling the water distribution within the gas diffusion layer of a fuel cell suggests a partial differential equation (PDE) approach. Starting from first principles, the model of a fuel cell is represented as a boundary value problem for a set of three coupled, nonlinear, second-order PDEs. These three PDEs are approximated, with justification rooted in linear systems theory and a time-scale decomposition approach, by a single nonlinear PDE. A hybrid set of numerical transient, analytic transient, and analytic steady-state solutions for both the original and single PDE-based model are presented, and a more accurate estimate of the liquid water distribution is obtained using the single PDE-based model. The single PDE derived represents our main contribution on which future development of control, estimation, and diagnostics algorithms can be based.**

I. Introduction and Motivation

Fuel cell technology holds significant promise for clean and renewable power generation for both stationary and mobile applications. Of critical importance to the efficient and long-life operation of a fuel cell system are:

- Maintaining humidity in a narrow range near water vapor saturation at the membrane while avoiding excess accumulation of liquid water in the channels (flooding).
- Keeping sufficient reactant concentration at the membrane to avoid starvation.

Due to a lack of direct measurements of the critical variables at the membrane and the channels, a low-order and compact model of the multi-component (reactants, water), two-phase (vapor and liquid water), spatially-distributed and dynamic behavior across the gas diffusion layer (GDL) (Fig. 1) is needed for estimation and control. The time-varying constituent distributions in the GDL of each electrode are described by three second-order parabolic PDEs for reactant (oxygen in the cathode and hydrogen in the anode) concentration, water vapor concentration, and liquid water volume. The electrochemical reactions on, and the mass transport through, the catalyst-covered membrane couple the anode and cathode behaviors and, together with the channel conditions, provide the time-varying boundary values for these PDEs.

The water (liquid and vapor) PDEs are strongly coupled through the evaporation/condensation rate. Further, the liquid water becomes a nonlinearly distributed parameter that inhibits reactant gas and water vapor diffusion. Specifically, liquid water occupies pore space in the GDL, impedes the diffusion of reactant flow towards the membrane, and ultimately reduces the active fuel cell area [1], causing performance degradation.

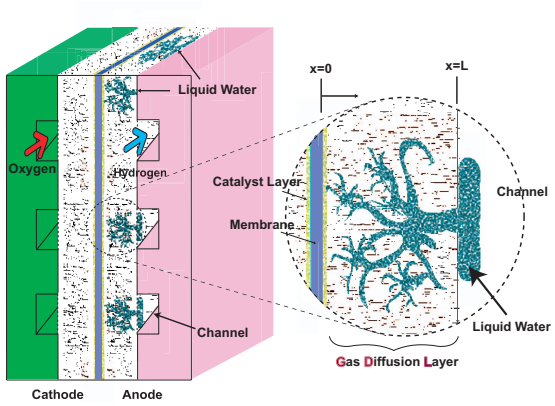

Fig. 1. Conceptual schematic showing accumulation of liquid water in the GDL and subsequent flow to the channel where reactant-blocking film is formed

Removal of accumulated liquid water is necessary to regain performance, which is typically accomplished by surging an inlet flow (e.g. anode H_2 supply). Allowing liquid water to accumulate is undesirable for performance, efficiency, and membrane durability reasons, hence it is clear that estimation and control of the liquid water distribution is critical for effective fuel cell management.

Previous work has used a set of twelve difference equations to approximate the six second-order PDEs of the model from [1]. Simulation using numerical integration showed reasonable matching to experimental data obtained from a 2.5 kW peak power stack of 24 fuel cells with 300 cm^2 active area. The numerical model was able to predict the stack voltage behavior during anode flooding which occurs at low and low-medium loads typical of operating modes in fuel cell vehicles. Despite the good prediction, the numerical model in [1] is complex and requires numerous simulations to gain insight of the dominant model parameters and dynamics.

In this paper we demonstrate using modal analysis that the gas and water vapor states have much faster response times than the liquid water states. This fact allows the use of the water vapor steady-state solution within the liquid water PDE to account for the evaporation/condensation coupling. Moreover, we show that the gas diffusion is not very sensitive to the distribution of liquid water (when liquid water is present) and a reasonable estimated value for the liquid water fraction is used to decouple the reactant and water vapor PDEs from the liquid PDE. Then analytic solutions of the

B.A. McCain, A.G. Stefanopoulou, and I.V. Kolmanovsky (bmccain, annastef, ilya@umich.edu) are with the Fuel Cell Control Laboratory, Mechanical Engineering Dept., University of Michigan.

Funding is provided from NSF-GOALI CMS-0625610.

anode reactant and the water vapor concentrations are derived using the net membrane water transport, which allows us to study the anode GDL phenomena without having to solve for the cathode liquid water distribution (and vice versa).

With the analytic solutions in hand, the liquid water distribution is governed by a single nonlinear PDE. This simplified model can greatly facilitate and enable future studies of control, estimation, and diagnostics problems from a rigorous control of PDEs perspective.

II. Model of the Anode Gas Diffusion Layer

We proceed with a one-dimensional treatment of the anode GDL processes, letting x denote the spatial variable, with x=0 corresponding to the membrane location and x=L corresponding to the channel location, and we let t denote the time variable.

The state variables are as follows:

- $c_{H_2}(x,t)$ is the hydrogen concentration (mol/m^3) at time t at a cross-section of the GDL located at x, $0 \le x \le L$;
- $c_{v,an}(x,t)$ is the concentration of water vapor at time t at a cross-section of GDL located at x, $0 \le x \le L$;
- $s(x,t)$ is the fraction of liquid water volume V_L to the total pore volume V_p, $s = \frac{V_L}{V_p}$. s is thus a concentration-like variable for the liquid water at time t, at a cross-section of GDL located at x, $0 \le x \le L$.

The following intermediate variables are useful:

- $N_{H_2}(x,t)$ is the hydrogen molar flux (mol/m^2/s) at time t at a cross-section of the GDL located at x, $0 \le x \le L$;
- $N_v(x,t)$ is the water vapor molar flux (mol/m^2/s) at time t at a cross-section of the GDL located at x, $0 \le x \le L$;
- $W_l(x,t)$ is the liquid water mass flow (kg/s) at time t at a cross-section of the GDL located at x, $0 \le x \le L$;

The molar fluxes are driven entirely by the presence of a concentration gradient (i.e. diffusion), since bulk flow (convection) is neglected:

$$N_{H_2} = -D_{H_2}(s)\frac{\partial c_{H_2}}{\partial x}, \qquad N_v = -D_v(s)\frac{\partial c_{v,an}}{\partial x}, \quad (1)$$

where $D_{H_2}(s)$ and $D_v(s)$ are effective diffusivities for hydrogen and water vapor which depend on the liquid fraction, s. Liquid water in the GDL occupies pore space, reducing the diffusivity, $D_j(s) = D_{\varepsilon,j}(1-s)^m$. Here $D_{\varepsilon,j}$ is a constant that depends on GDL porosity (ε), and $m = 2$ based on [2].

The gas constituent conservation equations are,

$$\frac{\partial c_{H_2}}{\partial t} = -\frac{\partial N_{H_2}}{\partial x}, \qquad \frac{\partial c_{v,an}}{\partial t} = -\frac{\partial N_v}{\partial x} + r_v(c_{v,an}), \quad (2)$$

where r_v is the evaporation rate defined as,

$$r_v(c_{v,an}) = \begin{cases} \gamma\left(c_{v,sat} - c_{v,an}\right) & \text{for } s > 0, \\ \min\left\{0, \gamma(c_{v,sat} - c_{v,an})\right\} & \text{for } s = 0 \end{cases}$$

where γ is the volumetric condensation coefficient and $c_{v,sat}$ is the vapor saturation concentration. Note that evaporation can only occur if there is liquid water ($s > 0$) in the GDL.

Under the isothermal conditions assumed for the anode GDL in this model, once the production or transport of vapor exceeds the ability of the vapor to diffuse through the GDL to the channel, the vapor supersaturates and condenses. The mass flow of liquid water is driven by the gradient in capillary pressure (p_c) due to build-up of liquid in the porous medium,

$$W_l = -\varepsilon A_{fc}\rho\frac{KK_{rl}}{\mu_l}\frac{\partial p_c}{\partial x}, \quad (3)$$

where μ_l is the liquid viscosity, A_{fc} (m^2) is the fuel cell active area, and K is the material-dependent absolute permeability. The relative liquid permeability $K_{rl} = \left(\frac{s-s_{im}}{1-s_{im}}\right)^3$, and the capillary pressure p_c (Pa) is a fitted third-order polynomial in s, the liquid water fraction. The condensed liquid accumulates in the GDL until it has surpassed the immobile saturation threshold (s_{im}), at which point capillary flow will carry it to an area of lower capillary pressure (toward the GDL-channel interface). The immobile water saturation s_{im} works as stiction, i.e. there is no liquid flow unless the liquid water fraction exceeds s_{im}. To facilitate the analytic solution, and express the equation in the physical variable s, (3) is rewritten as,

$$\begin{aligned} W_l &= -\varepsilon A_{fc}\rho_l\frac{K}{\mu_l}\left(\frac{s-s_{im}}{1-s_{im}}\right)^3\frac{dp_c}{ds}\frac{ds}{dx} \\ &\approx -\varepsilon A_{fc}\rho_l\kappa_\mu(s)\frac{ds}{dx}, \end{aligned} \quad (4)$$

using an approximation $\kappa_\mu(s) = \frac{b_1}{1-s_{im}}\left(\frac{s-s_{im}}{1-s_{im}}\right)^{b_2}$, where b_1 and b_2 are fitted parameters, and this approximation is only valid when $s > s_{im}$.

Conservation of liquid mass is employed to determine the rate of liquid accumulation,

$$\frac{\partial s}{\partial t} = -\frac{1}{\varepsilon A_{fc}\rho_l}\frac{\partial W_l}{\partial x} - \frac{M_v}{\rho_l}r_v(c_{v,an}), \quad (5)$$

where M_j is the molar mass of constituent j.

Combining (1) with (2) provides the two second-order parabolic PDEs that govern the reactant and water vapor concentrations,

$$\frac{\partial c_{H_2}}{\partial t} = \frac{\partial}{\partial x}\left(D_{H_2}(s)\frac{\partial c_{H_2}}{\partial x}\right), \quad (6)$$

and

$$\frac{\partial c_{v,an}}{\partial t} = \frac{\partial}{\partial x}\left(D_v(s)\frac{\partial c_{v,an}}{\partial x}\right) + r_v(c_{v,an}). \quad (7)$$

A similar result is found from (4) and (5) for the liquid water fraction PDE,

$$\frac{\partial s}{\partial t} = \frac{\partial}{\partial x}\left(\kappa_\mu(s)\frac{\partial s}{\partial x}\right) - \frac{M_v}{\rho_l}r_v(c_{v,an}). \quad (8)$$

The boundary conditions depend on the controllable outlet valve that determines the flow out of the anode channel, and on the disturbance input which is the current density drawn from the fuel cell, $i(t)$ (A/m^2).

For $c_{H_2}(x,t)$, mixed Neumann-Dirichlet (Robin) type boundary conditions are imposed. The channel (ch) boundary condition is,

$$c_{H_2}|_{x=L} = c_{H_2,ch} = p_{H_2,ch}/\left(RT\right), \tag{9}$$

where R is the universal gas constant, T is the temperature, and the hydrogen partial pressure in the anode channel, $p_{H_2,ch}$, depends on the control input, $u(t)$, as discussed in Sec. III. The membrane (mb) boundary condition is,

$$\left.\frac{\partial c_{H_2}}{\partial x}\right|_{x=0} = -\frac{1}{D_{H_2}(s)|_{x=0}} \cdot \frac{i(t)}{2F} = -\frac{N_{H_2,rct}}{D_{H_2}(s)|_{x=0}}, \tag{10}$$

where the rct subscript indicates the reaction of H_2 at the anode catalyst, which depends on the current density i, and F is Faraday's constant.

For $c_{v,an}(x,t)$, similar Robin boundary conditions are imposed:

$$c_{v,an}|_{x=L} = c_{v,an,ch} = p_{v,an,ch}/\left(RT\right), \tag{11}$$

$$\left.\frac{\partial c_{v,an}}{\partial x}\right|_{x=0} = \frac{-N_{mb}}{D_v(s)} = \beta_w(c_{v,ca} - c_{v,an})|_{x=0} - k_{v,0}\cdot i(t), \tag{12}$$

where β_w is a stack temperature-dependent parameter (influenced by membrane material properties, humidity, and active area) that is adapted from the back diffusion membrane water transport phenomenon in [3], and $k_{v,0}$ is a function of the unknown membrane water transport. We use a constant $k_{v,0}$ and justify this assumption in Sec. V-B.

Finally, for $s(x,t)$, Robin boundary conditions are again imposed. Specifically, since water passing through the membrane and into the GDL is in vapor form,

$$\left.\frac{\partial s}{\partial x}\right|_{x=0} = 0. \tag{13}$$

Since liquid water will be drawn away from the GDL due to its hydrophobic nature ([2]),

$$s(t,L) = s_{im}. \tag{14}$$

III. Anode Channel Equations

For the anode channel calculations the governing equations for hydrogen and water are:

$$\begin{aligned} dm_{H_2,ch}/dt = &\quad (W_{H_2,in} - W_{H_2,out} + W_{H2,GDL}),\\ dm_{w,ch}/dt = &\quad (W_{w,GDL} - W_{v,out}), \end{aligned} \tag{15}$$

where the anode inlet flow is dry hydrogen, $W_{H_2,in} = k_{an,in}(p^*_{an} - p_{an,ch})$ with $k_{an,in}$ as the proportionality constant for the error-driven pressure regulator used to determine inlet flow rate such that $p_{an,ch}$ tracks the reference pressure p^*_{an}. This reference is typically set near the cathode pressure for membrane safety.

The H_2 and water vapor partial pressures, which represent the channel boundary conditions, are calculated from:

$$\begin{aligned} p_{H_2,ch} &= \tfrac{m_{H_2,ch}RT}{M_{H_2}V_{ch}},\\ p_{v,an,ch} &= \min\left\{\tfrac{m_{w,ch}RT}{M_vV_{ch}}, p_{v,sat}\right\},\\ p_{an,ch} &= p_{H_2,ch} + p_{v,an,ch}. \end{aligned} \tag{16}$$

The anode exit flow rate to the ambient (amb),

$$W_{an,out} = u \cdot k_{an,out}(p_{an,ch} - p_{amb}), \tag{17}$$

is a controllable valve flow $0 \le u(t) \le 1$ for anode gas to remove both water, and unfortunately, hydrogen,

$$\begin{aligned} W_{H_2,out} &= \frac{m_{H_2,an,ch}}{m_{an,ch}}W_{an,out},\\ W_{v,out} &= W_{an,out} - W_{H_2,out}, \end{aligned} \tag{18}$$

where $m_{an,ch} = m_{H_2,an,ch} + p_{v,an,ch}V_{an}M_v/(RT)$. The hydrogen and water mass flow rate from the GDL to the anode are calculated using:

$$W_{H_2,GDL} = -\varepsilon A_{fc} M_{H_2}\left(D_{H_2}(s)\frac{\partial c_{H_2}}{\partial x}\right)\Bigg|_{x=L}, \tag{19}$$

$$W_{w,GDL} = -\varepsilon A_{fc}\left(\rho_l\kappa_\mu(s)\frac{\partial s}{\partial x} + M_vD_v(s)\frac{\partial c_{v,an}}{\partial x}\right)\Bigg|_{x=L}.$$

IV. Numerical Solution Analysis

In previous work [1], [4], [5], the one-dimensional system of interconnected parabolic PDEs of (6)-(8), combined with three similar PDEs describing the spatial and temporal evolution of the cathode oxygen reactant O_2, water vapor, and liquid fraction was modeled and discretized. The model was parameterized using data from an experimental fuel cell [1]. The discretized model was then used for model order reduction studies [4], [5]. A portion of the findings of these studies is summarized next because it is instrumental in condensing three coupled PDEs (6)-(8) to one parabolic PDE for the liquid fraction as shown in Sec. V.

A. System Discretization

It is because the boundary conditions for each of the constituents include a Neumann type that the discretization is performed on three pairs of first-order DEs (1)-(4) instead of on three second-order PDEs.

The forward-difference method is used for the discretizations of the flux and flow equations,

$$N_{H_2}(k) \simeq -D_{H_2}(s)\frac{c_{H_2}(k+1) - c_{H_2}(k)}{\delta x}, \tag{20}$$

$$N_v(k) \simeq -D_v(s)\frac{c_{v,an}(k+1) - c_{v,an}(k)}{\delta x}, \tag{21}$$

$$W_l(k) \simeq -\varepsilon A_{fc}\rho_l\kappa_\mu(s(k))\frac{s(k+1) - s(k)}{\delta x}, \tag{22}$$

where $\delta x = x(k+1) - x(k)$.

Next, since the fluxes across the membrane are included in the model, and form the boundary conditions, the difference equations relating the states to the fluxes are formed using the backward-difference method:

$$\frac{dc_{H_2}(k)}{dt} \simeq -\frac{N_{H_2}(k) - N_{H_2}(k-1)}{\delta x}, \tag{23}$$

$$\frac{dc_{v,an}(k)}{dt} \simeq -\frac{N_v(k) - N_v(k-1)}{\delta x} + r_v(c_{v,an}(k)), \tag{24}$$

$$\frac{ds(k)}{dt} \simeq -\frac{W_l(k) - W_l(k-1)}{\delta x} - \frac{M_v}{\rho_l}r_v(c_{v,an}(k)). \tag{25}$$

B. Time-Scale Decomposition

Insight into the relative response speeds of the system states is gained by linear time-scale decomposition techniques. Linearization of the 24-state system that resulted from the discretization of Sec. IV-A was performed around an operating point of $i = 0.25$A/cm^2, $T = 60^o$C, 100% saturated cathode inlet flow, and dry H_2 at the anode inlet. This operating point represents the midrange of the normal operation of the experimental fuel cell on which the model was tuned and consequently validated (i_{max} = 0.45 A/cm^2) [1].

Let **v** be the eigenevectors of the discretized and linearized system matrix A ($\dot{\mathbf{x}} = A\mathbf{x} + B\mathbf{u}$). The full fuel cell model (both anode and cathode) has 24 states that can be grouped as follows:

- Gas constituents in GDL: 13
- Liquid constituents in GDL: 6
- Gas constituents in channels: 5

We hypothesize that there is a similarity transformation $A_T = T^{-1}AT$ that will *practically* partition the system into two subsystems, one consisting only of gas states, and the other of only liquid states. This representation was accomplished by applying the balancing algorithm of [6], where each row-column pair of the system matrix A is scaled via similarity transformation T to have equal norms. This procedure generates a system of eigenvectors that are practically decoupled with $\mathbf{v}_T = T^{-1}\mathbf{v}$, and $V_T = [\mathbf{v}_{T,1}|\mathbf{v}_{T,2}|...|\mathbf{v}_{T,n}]$ defining the eigenspace of the transformed system. Normalizing those eigenvectors, and eliminating insignificant components, it is found that the eigenspace has the form:

$$V_T \approx \begin{bmatrix} 0 & V_{T,l,6\times 6} \\ V_{T,g,18\times 18} & 0 \end{bmatrix}, \qquad (26)$$

where the subscripts g and l indicate gas or liquid states. This shows that, though not a perfect mathematical decoupling, with reasonable thresholds a transformation can be found that results in a practical decoupling of the liquid and gas states. Note that the resulting eigenvectors cannot be associated with individual states of the original system, only that each eigenvector can be assigned to a linear combination of either only gas states or only liquid states.

The degree of gas/liquid coupling is tracked by the infinity norm of the set of V_T matrix elements that correspond to liquid states in the predominantly gas state eigenvectors plus the gas states in the predominantly liquid state eigenvectors. Using the same method, transformations for linearizations about the low and high end operating points showed that the strength of the gas/liquid coupling grows with the current density (i), though it does not exceed a negligible 2% at maximum current density (Table I).

TABLE I

GAS AND LIQUID STATE COUPLING VERSUS CURRENT DENSITY i.

i (A/cm)^2	0.10	0.25	0.45
Coupling	0.05%	0.3%	1.9%

Next, analysis of the eigenvalues indicated a two-order of magnitude gap between the minimum gas set eigenvalue and the maximum liquid set eigenvalue. The slow mode time constants (liquid) range from 7 to 132 seconds, while the fast modes (gas) have time constants ranging 0.32 ms to 0.14 sec.

This large scale separation indicates that the water vapor and H_2 concentrations reach equilibrium very fast, and thus the system behavior can be approximated with their steady-state solution when the goal is to control the liquid water accumulation. In our model simplification we thus need to maintain the temporal evolution of only the liquid water fraction PDE (5).

V. SIMPLIFIED MODEL

A study for the minimum necessary spatial discretization of the fuel cell dynamics model of [1], while maintaining the physical meanings of the states, was presented in [5]. Over-discretization was investigated using an energy-based metric known as *Activity* [7] to determine the degree of nonlinearity of a spatial gradient approximated by difference equations.

A key result of [5] was that the reduction of a 3-section liquid water discretization to a 1-section (i.e. lumped) approximation yielded very little degradation in cell output voltage prediction. Using the same methodology, the spatial distribution of the hydrogen concentration in the anode was found and confirmed to be linear (linearity is also confirmed in this work by the analytic solution found below). However, the same conclusion could not be reached for the water vapor concentration. In order to accurately predict the water vapor concentration at the membrane, a lumped-parameter approach was found to be unacceptable due to large error in membrane transport and GDL-channel water flow estimations.

A. Coupling Sensitivity of the Gaseous and Liquid States

There are two phenomena responsible for the coupling between the liquid and the gas states occurring in this system. The first is the direct coupling between water vapor concentration and liquid fraction due to evaporation/condensation, which is clear from (5). Second, the amount of liquid water present has an influence on the gas fluxes via the diffusivity's dependence on s (1).

The results of our numerical modeling indicate that with an assumption of constant diffusivity calculated using the average liquid water fraction, approximation errors are negligible, i.e. with $D_v(s_{avg}) = D_v \frac{1}{L}\int_0^L s(x)dx$). Since average liquid water fraction is, in general, unknown, a constant diffusivity calculated based on $s = s_{im}$, i.e. $D_v(s_{im})$, has been implemented instead and shown to produce a slightly deteriorated, but still acceptable, approximation. See, for instance, Fig. 2 which compares the prediction of the difference $(c_{v,an} - c_{v,sat})\big|_{x=0}$, which is a critical value for estimation of membrane water transport.

Note that the results of Sec. IV-B suggest that the diffusivities can be treated as time-invariant parameters for solving the gas PDEs due to the significant separation in time-scale relative to the liquid fraction PDE.

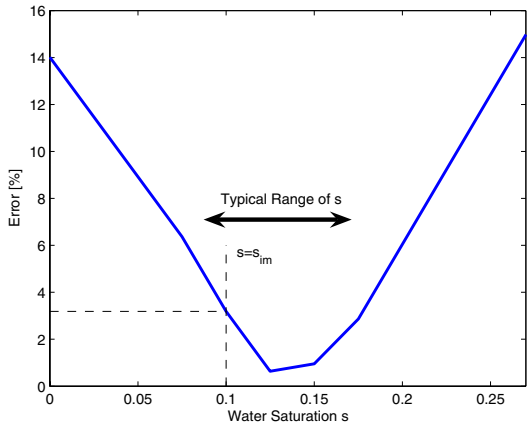

Fig. 2. Steady-state error in $(c_{v,an} - c_{v,sat})|_{x=0}$ for varying choices of constant liquid water fraction.

With the assumption of constant diffusivities, denoted $\bar{D}_v$ and $\bar{D}_{H_2}$ for the water vapor and H_2 cases respectively, it is possible to solve the $c_{H_2}(x,t)$ and $c_{v,an}(x,t)$ second-order PDEs analytically using separation of variables.

B. The Gas Constituent Solutions

Under the condition that the GDL is assumed to have liquid water present at all points x, i.e. $s > 0$ so that the evaporation reaction term is active, the solutions are:

$$c_{H_2}(x,t) = \sum_{n=0}^{\infty} e^{-\bar{D}_{H_2}\eta_n t} A_n \cos(\sqrt{\eta_n}x) + \frac{N_{H_2 rct}}{\bar{D}_{H_2}}(L-x) + c_{H_2,ch}, \quad (27)$$

$$c_{v,an}(x,t) = \sum_{n=0}^{\infty} e^{-\zeta_n t} B_n \cos(\sqrt{\eta_n}x) + (\alpha_1 e^{\beta x} + \alpha_2 e^{-\beta x}) + c_{v,sat}, \quad (28)$$

where

$$\eta_n = (n + 1/2)^2 \pi^2 / L^2, \quad (29)$$

and

$$\beta = \sqrt{\gamma/\bar{D}_v} \qquad \zeta_n = (\bar{D}_v \eta_n + \gamma). \quad (30)$$

Figure 3 shows the transitions from an initial distribution to the next steady-state distribution required due to a change in boundary conditions. The changes in slopes at the membrane are caused by a step current density input at $t = t_o = 0$ ms. The fast time constants derived in Sec. IV-B are apparent.

A_n and B_n are coefficients of the infinite series approximation for the shape of the distribution of the respective concentrations at time t = 0. For the H_2 solution, the coefficients A_n are

$$A_n = \frac{2}{L}\left[\frac{N_{H_2,rct}|_{t=0^-} - N_{H_2,rct}|_{t=0}}{\bar{D}_{H_2}\eta_n} + \frac{(-1)^n (c_{H_2,ch}|_{t=0^-} - c_{H_2,ch}|_{t=0})}{\sqrt{\eta_n}}\right]. \quad (31)$$

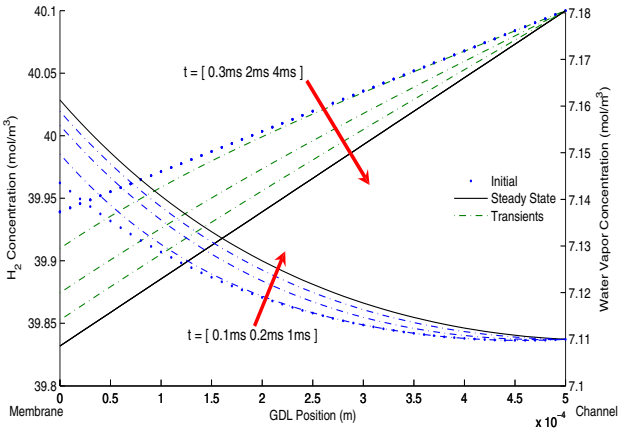

Fig. 3. Transient solutions of c_{H_2} and $c_{v,an}$ for a step in current density (0.15 $\rightarrow$ 0.30 A/cm^2).

From (28) it can be seen that the water vapor transient response solution is thus a transition from one exponential form steady-state solution to the next, described by the product of a decaying exponential in time and an infinite Fourier series. The coefficients for the water vapor transient solution are,

$$B_n = \frac{2}{L(\beta^2 + \eta_n)}[\beta(\phi_2 - \phi_1) + \sqrt{\eta_n}(-1)^n(\phi_1 e^{\beta L} + \phi_2 e^{-\beta L})], \quad (32)$$

where

$$\phi_i = \alpha_i|_{t=0} - \alpha_i|_{t=\infty}. \quad (33)$$

The α_i are functions of the membrane water vapor transport (N_{mb}) and the anode channel condition,

$$\begin{aligned} \alpha_1 e^{\beta L} + \alpha_2 e^{-\beta L} &= c_{v,an,ch} - c_{v,sat}, \\ \alpha_1 - \alpha_2 &= -N_{mb}/\beta\bar{D}_v. \end{aligned} \quad (34)$$

Determination of N_{mb} requires knowledge of the water vapor concentrations on both sides of the membrane, and since the water vapor PDE steady-state solution takes the form,

$$c_{v,e}(x) = \left(\alpha_1 e^{\beta x} + \alpha_2 e^{-\beta x}\right) + c_{v,sat}, \quad (35)$$

then,

$$\begin{aligned} c_{v,an,mb} &= (\alpha_1 + \alpha_2) + c_{v,sat} \\ c_{v,ca,mb} &= (\nu_1 + \nu_2) + c_{v,sat}, \end{aligned} \quad (36)$$

where the mb subscript signifies the value is taken at the membrane (x=0). The ν_i, similar to the α_i, are dependent upon N_{mb} and the cathode channel condition, but are additionally influenced by the water vapor reaction term $N_{v,rct} = \frac{i}{2F}$ from the reformation of H_2O at the cathode catalyst,

$$\begin{aligned} \nu_1 e^{-\beta L} + \nu_2 e^{\beta L} &= c_{v,ca,ch} - c_{v,sat} \\ \nu_1 - \nu_2 &= (-N_{mb} + N_{v,rct})/\beta\bar{D}_v. \end{aligned} \quad (37)$$

Finally, N_{mb} can be found from,

$$N_{mb} = \beta_w(c_{v,ca,mb} - c_{v,an,mb}) - \frac{i}{F}(0.0029\lambda_{mb}^2 + 0.05\lambda_{mb}), \quad (38)$$

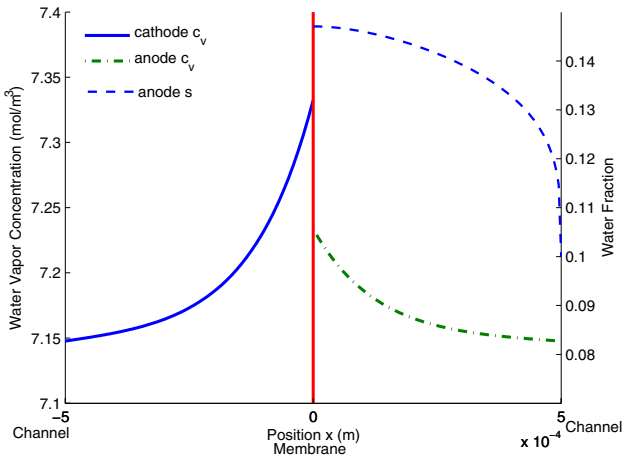

Fig. 4. Channel-to-channel steady-state solutions of $c_{v,ca}$, $c_{v,an}$, and the anode steady-state liquid water fraction solution $s(x)$, which displays strong nonlinearity as x $\rightarrow$ L.

where λ_{mb} is the water content of the membrane, and is a linear function of the average of $c_{v,ca,mb}$ and $c_{v,an,mb}$.

The second term on the right side of (38) can be very well approximated when humidity is near 100% by a linear function of i to enable simple matrix algebra solutions of (34)-(38) to be calculated online,

$$\frac{i}{F}(0.0029\lambda_{mb}^2 + 0.05\lambda_{mb}) \cong 1.512 \times 10^{-5} i. \qquad (39)$$

Figure 4 shows the steady-state solutions for water vapor concentrations in the anode and cathode GDLs found using the simultaneous system solution process. For reference, the steady-state solution for the liquid water fraction is also shown. We now have the ability to determine the net steady state water transport across the membrane using only channel boundary conditions.

C. Liquid Water Governing Equation

The liquid water distribution in the porous medium is obtained by substituting (4) into (5), and replacing the $c_{v,an}(x,t)$ coupling term by its steady-state solution (35) (since it has been shown that the time constant of the water vapor is multiple orders of magnitude faster than that of the liquid water),

$$\frac{\partial s}{\partial t} = \frac{\partial}{\partial x}\left(\kappa_\mu(s)\frac{\partial s}{\partial x}\right) + \frac{M_v}{\rho_l}\gamma(\alpha_1 e^{\beta x} + \alpha_2 e^{-\beta x}). \qquad (40)$$

This equation can be integrated twice to obtain the steady-state solution,

$$s_0(x) = \beta_z(\beta(\alpha_1 - \alpha_2)(x - L) + c_{v,an,ch} - c_{v,sat} - (\alpha_1 e^{\beta x} + \alpha_2 e^{-\beta x}))^{\frac{1}{b_2+1}} + s_{im}, \qquad (41)$$

where β and α_i are as defined in the $c_{v,an}(x,t)$ solution previously, and

$$\beta_z = (1 - s_{im})\left(\frac{\varepsilon A_{fc} M_v \gamma(b_2+1)}{\beta^2 b_1}\right)^{\frac{1}{b_2+1}}. \qquad (42)$$

For comparison to the original 24-state system, a numeric solution to the second-order difference equation is obtained by substituting (22) into (25), and using the steady-state vapor solution (35) for the evaporation/condensation term,

$$\frac{ds(k)}{dt} \simeq \frac{\Theta(k+1) - 2\Theta(k) + \Theta(k-1)}{\delta x^2} + \frac{M_v\gamma}{\rho_l}\left(\alpha_1 e^{\beta x(k)} + \alpha_2 e^{-\beta x(k)}\right), \qquad (43)$$

where $\Theta(k) = \int \kappa_\mu(s(k))ds$, and $\kappa_\mu(s)$ is as introduced in (4).

The explicit solution to (40) has yet to be found and we therefore implement the model based on (27), (28), and (43), and refer to it as a semi-analytic model.

Comparison to voltage prediction of the numeric model confirms that there is virtually no difference in the voltage predictive capability of the semi-analytic model versus the coarse numeric model. The voltage prediction model used requires significant explanation, and this, along with detailed results, will be discussed in future publications.

VI. Conclusions

A first principles model describing the reactant, water vapor, and liquid water dynamics in a polymer electrolyte membrane fuel cell anode GDL has been reduced to two analytic solutions (hydrogen and water vapor) and one second-order discretized PDE (liquid water) given by (43). Additionally, a method to simultaneously obtain the water vapor concentration analytic solutions across the membrane is provided so that solutions can be obtained using only channel variables. These two contributions enable fast and computationally inexpensive estimation of states within the GDL, as evidenced by a 36% reduction in simulation steps for identical experimental inputs and a 61% reduction in function calls. These improvements facilitate the next step of control of liquid water in the GDL to prevent voltage degradation.

References

[1] D. A. McKay, W. T. Ott, and A. G. Stefanopoulou, "Modeling, parameter identification, and validation of water dynamics for a fuel cell stack." Orlando, FL, USA: ASME Conference on Fuel Cell Science, Engineering and Technology, Nov 2005, FUELCELL2005-81484.

[2] J. H. Nam and M. Kaviany, "Effective diffusivity and water-saturation distribution in single- and two-layer pemfc diffusion medium," *Int. J Heat Mass Transfer*, vol. 46, pp. 4595–4611, 2003.

[3] T. Springer, T. Zawodzinski, and S. Gottesfeld, "Polymer electrolyte fuel cell model," *Journal of the Electrochemical Society*, 1991.

[4] B. A. McCain and A. G. Stefanopoulou, "Order reduction for a control-oriented model of the water dynamics in fuel cell stack systems." Irvine, CA, USA: ASME Conference on Fuel Cell Science, Engineering and Technology, June 2006, FUELCELL2006-97075.

[5] B. A. McCain, A. G. Stefanopoulou, and K. R. Butts, "A study toward minimum spatial discretizations of a fuel cell dynamics model." Chicago, IL, USA: ASME Int'l Mechanical Engineering Congress and Exposition, Nov 2006, IMECE2006-14509.

[6] E. Osborne, "On pre-conditioning of matrices," *Journal of the ACM*, pp. 338–345, 1960.

[7] L. Louca, J. Stein, G. Hulbert, and J. Sprague, "Proper model generation: An energy-based methodology," *Proceedings of the 1997 International Conference on Bond Graph Modeling*, pp. 44–49, 1997.